Electronic Supplementary Information (ESI)

Aptamer-modified Zr-MOFs to construct nanocatalysts with engineered specificity toward paraoxon

Tingwei Cao [a], Jiaxing Zhang [a] , Wei Qi [a,c,d] and Mengfan Wang *[,a,b,d]

a. School of Chemical Engineering and Technology, State Key Laboratory of Chemical Engineering, Tianjin University, Tianjin 300350, P. R. China.

b. School of Life Sciences, Tianjin University, Tianjin 300072, P. R. China.

c. The Co-Innovation Centre of Chemistry and Chemical Engineering of Tianjin, Tianjin 300072, P. R. China.

d. Tianjin Key Laboratory of Membrane Science and Desalination Technology, Tianjin 300350, P. R. China.

* Corresponding E-mail: mwang@tju.edu.cn (M. Wang)

SI Contents

1. Materials and methods

1.1 Chemicals and materials

Zirconium chloride ($ZrCl_4$), 2-amino-terephthalic acid (BDC-NH_2), N,N-dimethylformamide (DMF), 4-hydroxyethyl piperazine ethyl sulfonic acid (HEPES), phosphate buffer (PBS), sodium carbonate (Na_2CO_3), 4-aminoantipyrine (4-AAP), potassium ferricyanide ($K_3Fe(CN)_6$), 4-nitrophenyl phosphate disodium salt (PNPP) and p-nitrophenol (p-NP) were purchased from Aladdin (Shanghai, China). Paraoxon (PXN), profenofos (PFF), isoprocarb, carbaryl and parathion-methyl (PTM) were purchased from Anpel (Shanghai, China). Glacial acetic acid, methanol and ethanol were purchased from Jiangtian (Tianjin, China). Glutaraldehyde (2.5 wt% aqueous water) was purchased from Kemiou (Tianjin, China). Aptamer used in this work (**Table S4**) was purchased from Genewiz (Tianjin, China). All the chemicals and organic solvents were analytical pure, and water was ultrapure water.

1.2 Synthesis of UiO-66-NH_2

160 mg of $ZrCl_4$ and 124 mg of BDC-NH_2 were dissolved in 40 mL DMF. Then, 1.4 mL of glacial acetic acid was added. After ultrasonic treatment for 5 min, the mixture was transferred into a kettle and reacted at 120 °C for 48 h. After the reaction, the mixture was cooled to room temperature. The solid product was centrifuged and washed with DMF and methanol, respectively. Finally, the obtained UiO-66-NH_2 was dried in vacuum at 120 °C for 12 h.

1.3 Synthesis of UiO-66-APT

UiO-66-NH_2 was dispersed in 500 μL of deionized water to the concentration of 5 mg/mL. Then, 500 μL of glutaraldehyde (2.5 wt% in aqueous water) was added, and the reaction was carried out at room temperature for 2 h on a rotary oscillator at a speed of 50 r/min. Then, the supernatant was removed by centrifugation, and 400 μL of HEPES buffer (20 mM, pH7.4) and 100 μL of aptamer (2.5 μM in HEPES buffer) was added (the aptamer was pre-heated at 95 °C for 2 min). The reaction continued at 37 ℃ for 24 h, and the suspension was centrifuged, washed and re-dispersed with HEPES

buffer (20 mM, pH7.4) to obtain UiO-66-APT (UiO-66-5'C6, UiO-66-5'C12 and UiO-66-3'C7), and finally stored at 4 °C for future use. The amount of aptamer that conjuncted on UiO-66-APT can be obtained through determining the content of aptamer in the supernate before and after modification.[1]

1.4 Catalytic ability evaluation

960 μL of HEPES buffer (20 mM, pH8.0), 20 μL of 20 mM PNPP solution, 20 μL of catalysts suspension (5 mg/mL) were mixed evenly and the reaction was carried out at 37 °C. During the reaction, the UV spectrum scanning of 300 ~500 nm was measured. The amount of p-NP in supernatant was determined at the wavelength of 400 nm. As the blank, PNPP was replaced with 20 μL of water.

For the hydrolysis of PXN, the above process was repeated by replacing 20 mM PNPP solution with 1 mg/mL PXN solution (PXN was pre-dissolved in acetone). Similarly, in the blank group, 20 μL of PXN solution was replaced by 20 μL of acetone solution. Kinetic fitting was carried out according to the experimental results.

The determination of PTM hydrolysis required the addition of 20 μL of 10% Na_2CO_3 solution as a chromogenic agent, and then detected at 450 nm.[2] For PFF, 960 μL of HEPES buffer (20 mM, pH7.0) was used instead of HEPES buffer (20 mM, pH8.0). After the reaction, 20 μL of 1.0% 4-AAP solution and 10 μL of 2.0% $K_3Fe(CN)_6$ solution were added as the chromogenic reagents, and then detected at 509 nm.[3] For isoprocarb, PBS buffer (20 mM, pH7.4) was used instead of HEPES buffer (20 mM, pH8.0). Then the fluorescence intensity at 281 nm before and after the hydrolysis reaction was measured at 252 nm excitation wavelength.[4] For carbaryl, HEPES buffer (20 mM, pH7.4) was used instead of HEPES buffer (20 mM, pH8.0). Then, the fluorescence intensity at 616 nm before and after the hydrolysis reaction was measured at the excitation wavelength of 310 nm.[5]

1.5 Characterizations

Scanning electron microscopy (SEM) S4800 was used to determine the morphology. Transmission electron microscopy (TEM) images were performed with a electron microscope (JEM-2100F, Japan). Elemental mapping was carried out using the

same electron microscope equipped with an energy dispersive X-ray spectrometer. The powder X-ray diffraction (XRD) patterns were collected on a D8-Focus X-ray diffractometer with Cu-Kα radiation and a scanning speed of 8 °/min. UV-visible spectra (UV) was measured on a TU-1900 spectrophotometer. A Nicolet 6700 spectrometer was employed to collect the Fourier-transform infrared (FT-IR) spectra, in KBr particles at room temperature over the range of 500~4000 cm^{-1}. X-ray photoelectron spectroscopy (XPS) data was collected using a Thermo Scientific K-Alpha+ photoelectron spectrometer equipped with an Al Ka X-ray source (1486.6 eV).

1.6 Molecular dynamics simulation

The molecular dynamics (MD) simulation was performed using the GROMACS 2021.3 software package[6] under the Amber ff99SB force field.[7] Based on the optimized crystal structure, the topological structure of UiO-66-NH_2 was generated by Sobtop program.[8] The PXN aptamer models were constructed based on the secondary structure, assembled with alkyl linker and finally connected onto UiO-66-NH_2 by glutaraldehyde to form UiO-66-APT. Then the simulation systems were established by expanding the UiO-66-APT structure with a margin of 0.8 nm. Substrate molecules were randomly inserted, and the boxes were filled with TIP3P water.[9] Moderate Na^+ ions were added to equilibrate the systems. Afterward, energy-minimization was accomplished in 5000 steps with the steepest descendant algorithm, followed by 100 ps equilibration stage and 2 ns production simulation stage under the NPT ensemble. In a simulation system, the UiO-66-ATP model was established through uniformly connecting appropriate aptamer to a UiO-66-NH_2 cell. Then, PXN molecules were randomly inserted into each system (the number of aptamer and PXN in each system was 1 : 1). The statistical mean distance was calculated every 1 ps from 0 to 2 ns for the entire locus. The average distance between the PXN molecules and the catalytic active center was calculated by taking the first 100 of the minimum median distances. The atoms within the whole UiO-66-ATP were selected for evaluating the radius of gyration. Finally, the conformations were observed and analyzed by Visual Molecular Dynamics (VMD),[10] MD analysis python package[11] and GROMACS analysis tools.

2. Supporting Figures

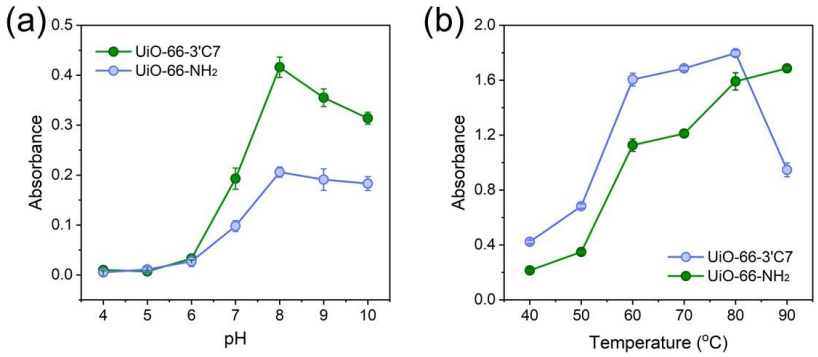

Fig. S1 The catalytic ability of UiO-66-NH_2 and UiO-66-3'C7 on PXN under different pH (a) and temperature (b) conditions.

960 μL of HEPES buffer (20 mM), 20 μL of 0.5 mg/mL PXN solution, 20 μL of catalysts suspension (5 mg/mL) were mixed evenly. The reaction was kept for 30 min under different pH or temperature conditions, then the absorbance of the reaction solution at 400 nm was determined.

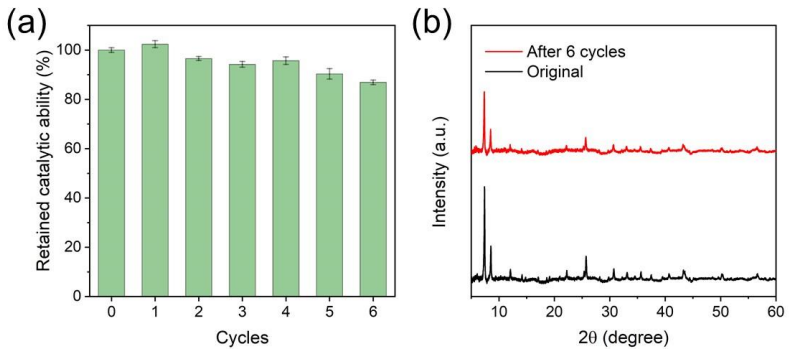

Fig. S2 The reusability of UiO-66-3'C7 (a). The XRD of original UiO-66-APT and recycled after 6 times (b).

960 μL of HEPES buffer (20 mM, pH8.0), 20 μL of 1 mg/mL PXN solution, 20 μL of UiO-66-3'C7 suspension (5 mg/mL) were mixed evenly. The reaction was kept for 30 min under 37 °C, then the absorbance of the reaction solution at 400 nm was determined. Assuming the original catalytic ability of UiO-66-3'C7 as 100%. After each catalytic cycle, the catalyst was centrifuged from the reaction solution, washed with deionized water, and then immersed in a fresh substrate solution for the next cycle. It can be seen

from **Fig. S2** that after 6 cycles, UiO-66-3'C7 still retained 87 % of the catalytic ability. This high stability is beneficial from the rigid crystal structure of the MOFs.

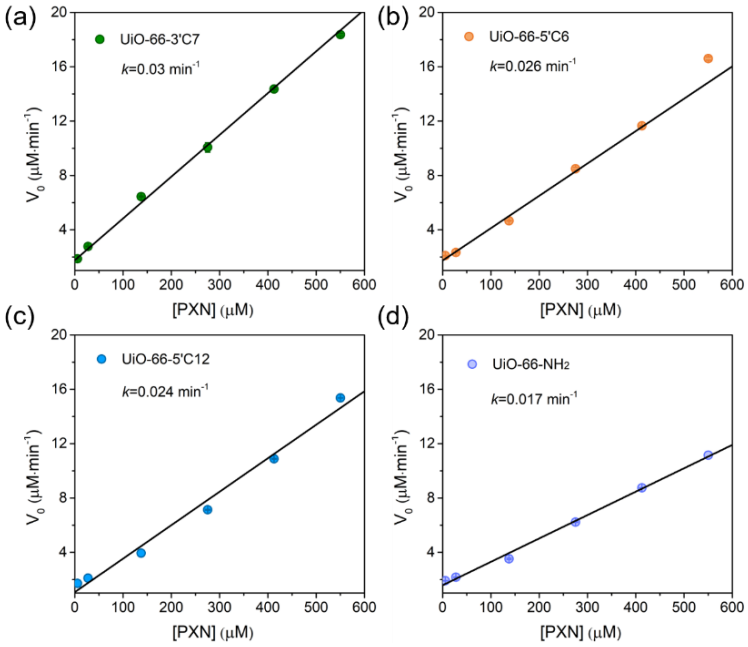

Fig. S3 The reaction rate versus PXN concentration plots.

3. **Supporting Tables**

Table S1. Element content results obtained from EDS-mapping test.

UiO-66-NH_2				
Element	Line type	Mass (%)	Wt % Sigma	Atom (%)
C	K	76.02	0.75	82.26
O	K	19.27	0.47	15.65
Zr	L	2.91	0.23	0.41
N	K	1.80	0.76	1.67
P	K	0.00	0.07	0.00
Total		100.00		100.00
UiO-66-5′C6				
Element	Line type	Mass%	Wt % Sigma	Atom%
C	K	74.40	1.01	82.53
O	K	17.42	0.58	14.51
Zr	L	5.86	0.42	0.86
N	K	2.11	1.04	2.01
P	K	0.21	0.14	0.09
Total		100.00		100.00

Table S2. The amount of aptamer conjunted on UiO-66-APT.

Nanocatalysts	Aptamer amount (mg/g)	Aptamer amount obtained from ICP OES (mg/g)
UiO-66-3’C7	8.77	9.13
UiO-66-5’C6	9.29	9.43
UiO-66-5’C12	8.40	9.05

Table S3. Radius of gyration results of UiO-66-APT.

Nanocatalysts	**UiO-66-3′C7**	**UiO-66-5′C6**	**UiO-66-5′C12**
Radius of gyration (nm)	118	80	100

Table S4. Sequences of aptamer conjuncted onto UiO-66-NH_2.

APT	Aptamer sequence
3'C7	5'-AAGCTTGCTTTATAGCCTGCAGCGATTCTTGATCGGAAAAGGCT GAGAGCTACGC-**-$(CH_2)_7$-NH_2-3'**
5'C6	**5'-NH_2-$(CH_2)_6$-**AAGCTTGCTTTATAGCCTGCAGCGATTCTTGATCGG AAAAGGCTGAGAGCTACGC-3'
5'C12	**5'-NH_2-$(CH_2)_{12}$-**AAGCTTGCTTTATAGCCTGCAGCGATTCTTGATCGG AAAAGGCTGAGAGCTACGC-3'

References

1 Y. Ouyang, Y. Biniuri, M. Fadeev, P. Zhang, R. Carmieli, M. Vázquez-González and I. Willner, *Journal of the American Chemical Society*, 2021, **143**, 11510-11519.

2 W. Lan, G. Chen, F. Cui, F. Tan, R. Liu and M. Yushupujiang, *Sensors (Basel)*, 2012, **12**, 8477-8490.

3 X. Tan, W. Xie, Q. Jia, F. Zhao, W. Wu, Q. Yang and X. Hou, *Analyst*, 2022, **147**, 4105-4115.

4 S. Wang, X. Wang, X. Chen, X. Cao, J. Cao, X. Xiong and W. Zeng, *RSC Advances*, 2016, **6**, 46317-46324.

5 Y. Han, Z. Ye, F. Wang, T. Chen, L. Wei, L. Chen and L. Xiao, *Nanoscale*, 2019, **11**, 14793-14801.

6 M. J. Abraham, T. Murtola, R. Schulz, S. Páll, J. C. Smith, B. Hess and E. Lindahl, *SoftwareX*, 2015, **1-2**, 19-25.

7 C. Tian, K. Kasavajhala, K. A. A. Belfon, L. Raguette, H. Huang, A. N. Migues, J. Bickel, Y. Wang, J. Pincay, Q. Wu and C. Simmerling, *J Chem Theory Comput*, 2020, **16**, 528-552.

8 A. W. Sousa da Silva, Vranken, W.F, *BMC Res Notes*, 2012, **5**, 367-374.

9 W. L. Jorgensen, J. Chandrasekhar, J. D. Madura, R. W. Impey and M. L. Klein, *The Journal of Chemical Physics*, 1983, **79**, 926-935.

10 H. William, D. Andrew and S. Klaus, *Journal of Molecular Graphics*, 1996, **14**, 33-38.

11 N. Michaud-Agrawal, E. J. Denning, T. B. Woolf and O. Beckstein, *J Comput Chem*, 2011, **32**, 2319-2327.